



Gas transport properties of novel mixed matrix membranes made of titanate nanotubes and PBI or PPO

V. Giel^{a,*}, B. Galajdová^a, D. Popelková^a, J. Kredatusová^a, M. Trchová^a, E. Pavlova^a, H. Beneš^a, R. Válek^b, J. Peter^a

^aInstitute of Macromolecular Chemistry, Academy of Sciences of the Czech Republic, Heyrovsky Sq. 2, 162 06 Prague 6, Czech Republic, Tel. +420 296809245; Fax: +420 296809410; email: guel@imc.cas.cz (V. Giel), Tel. +420 296809247; email: galajdova@imc.cas.cz (B. Galajdová), Tel. +420 296809225; email: popelkova@imc.cas.cz (D. Popelková), Tel. +420 296809293; email: kredatusova@imc.cas.cz (J. Kredatusová), Tel. +420 296809381; email: trchova@imc.cas.cz (M. Trchová), Tel. +420 296809367; email: pavlova@imc.cas.cz (E. Pavlova), Tel. +420 296809421; email: benesh@imc.cas.cz (H. Beneš), Tel. +420 296809246; email: peter@imc.cas.cz (J. Peter)

^bMembrain s.r.o., Pod Vinicí 87, 471 27 Stráž pod Ralskem, Czech Republic, Tel. +420 60155629; email: robert.valek@membrain.cz

Received 28 July 2014; Accepted 7 October 2014

ABSTRACT

Titanate nanotubes (TiNTs) for enhancing the gas separation performance of mixed matrix membranes (MMMs) are addressed in this work. The incorporation of different amount of TiNT into commercially available polymers such as polybenzimidazole (PBI) and poly(2,6-dimethyl-1,4-phenylene oxide) (PPO) was successfully carried out. The structure and properties of the MMMs were examined using scanning electron microscope (SEM), infrared spectroscopy (IR), and thermogravimetric analysis (TGA). From SEM studies, it was found that the membranes are homogenous and the nanotubes are well distributed in the polymer matrix. The IR spectra showed that PBI interacts with the nanotubes, whereas interaction of PPO with TiNT has not been observed. TGA measurements of PBI-TiNT membranes showed an increase of thermal stability with a higher content of TiNT, whereas no influence of TiNT in PPO membranes is ascertainable. The content of TiNT in membranes affects also the gas transport properties which were investigated with a time lag permeation apparatus and a sorption balance. It is shown that the presence of the TiNT increases the permeability coefficients of H₂, CO₂, O₂, N₂, and CH₄ in the PPO-TiNT membranes and decreases these values in the PBI-TiNT membranes. The obtained results of the separation showed that 6 wt.% of TiNT in PBI gave a rise to H₂/N₂ and CO₂/N₂ selectivities of 603 and 62 with H₂ and CO₂ permeabilities of 0.92 and 0.068 Barrers, respectively. PPO-TiNT MMM declined the CO₂/CH₄ selectivity to a value of 13 with a CO₂ permeability of 156 Barrer. Sorption isotherms exhibited nonlinear “dual-sorption” behavior for all gasses. The presence of TiNT in PBI matrix increases CO₂ sorptions, whereas influence on other gasses is less noticeable.

Keywords: Polybenzimidazole; Poly(phenylene oxide); Titanate nanotubes; Mixed matrix membrane; Gas separation; Permeability; Sorption isotherms

*Corresponding author.

Presented at the MELPRO 2014 Conference Membrane and Electromembrane Processes, 18–21 May 2014, Prague, Czech Republic

1. Introduction

Nowadays, separation of gasses via membranes is a widespread method in the industry for ammonia purge gas separation, hydrogen recovery, or nitrogen generation [1]. Each application needs a membrane of a specific material. Extensive research has been conducted on polymeric materials such as glassy or rubbery polymers for the use in membranes. Whereas glassy polymers generally exhibit high selectivities and low permeabilities, rubbery polymers exhibit higher permeabilities but lower selectivities. As Robeson's upper bound curves show [2,3], polymer membranes possess a trade-off between permeability and selectivity; wherefore researchers explored the influence of inorganic fillers of these membranes [4,5]. Thus far, a large variety of organic–inorganic composites have been reported [5–9]. Following several assumptions regarding features of fillers have been done: The fillers should possess either great gas adsorption or molecular sieving properties, and the fillers should be dispersed and distributed well in a continuous polymeric matrix. Usual fillers for embedding in the polymer matrix are for instance metal organic frameworks, mesoporous silicas, metal peroxides, carbon molecular sieves, or carbon nanotubes (CNTs) [5].

CNT arouse great excitement in the center of scientists' attention and seems to be a promising solution to overcome Robeson's upper bound because of their unique tubular structure of nanometer diameter and large length/diameter ratio [10]. CNTs can be either randomly arranged in the polymer matrix and build a non-woven, paper-like structure with a large specific surface area or aligned and create pathways in the membrane and hence increase the flux of gasses through the membrane [11]. Kim et al. reported increased permeability of O₂, N₂, and CH₄ proportionally to the amount of open-ended CNTs in the polymer matrix [5]. Sharma and coworkers prepared nanocomposites from polycarbonate and single-wall carbon nanotubes (SWNT) as well as multiwall carbon nanotubes (MWNT). They observed that the permeability for H₂ gas increases in aligned SWNT/PC and MWNT/PC nanocomposites in comparison to random oriented SWNT/PC and MWNT/PC [12]. Cong and his group incorporated SWNT and MWNT into brominated poly(2,6-dimethyl-1,4-phenylene oxide) (PPO) for the separation of CO₂/N₂. It was found that the composite membranes had an increased CO₂ permeability, while the CO₂/N₂ selectivity was similar to the neat polymer membrane. Furthermore, permeability increased with the amount of CNT [13].

Thus far, the most studied fillers are CNT. Nevertheless, it exists a number of other types of nanotubes made of non-carbon materials. Recent developments have shown promising features of titanate nanotubes (TiNT) as an additive to develop new materials, due to their tubular structure and simple synthesis at low temperature [14]. However, the process how to influence the material properties based on TiNT is not understood yet [15]. Those non-CNT might play an important role for membrane processes in the future. Based on this context, this work focuses on TiNT, which is synthesized at the Institute of Macromolecular Chemistry in Prague in high quality and gram quantities. Those nanotubes are 10 nm in diameter and 100–1,000 nm long as the morphology studies showed [16]. New mixed matrix membranes (MMMs) were prepared based on those nanotubes and the commercially available, high permeable polymers PPO and polybenzimidazole (PBI). Although a lot of studies have been done on those polymers, there is still a large room for improvement of membranes based on PPO and PBI. The present work aims to investigate the effect of TiNT on the morphology and performance of PPO and PBI membranes. It is expected through embedding of the nanotubes that the selectivities increase because the diameter of the fillers is bigger than the size of the gas molecules. Therefore, the gas molecules such as H₂, O₂, N₂ can also adsorb in the nanotube and at the same time permeate through the polymer.

In this article, first, the morphology and physico-chemical properties of MMMs are presented. Second, the influence of TiNT on gas transport is discussed. Third, the effect of polymer–nanotube ratio (1.5, 3, 6, and 9 wt.%) on permeability and selectivities is discussed.

2. Experimental details

2.1. Materials

PPO was supplied by Spolana Neratovice (Czech Republic). The molecular weight was determined by light scattering and average out at $M_w = 208,000$. Chloroform (stabilized with Amylene, Lachner, Czech Republic) was used for dissolving PPO.

PBI, full chemical name poly(5,5-bisbenzimidazole-2,2-diyl-1,3-phenylene), (Hoechst Celanese) was used as received as a 10% N,N-dimethylacetamide (DMAc) solution with a lithium chloride content of ~2%.

TiNT were synthesized by hydrothermal treatment. 0.2 g of TiO₂ powder (rutile modification, Sigma-Aldrich) was added to 200 ml of 10 M NaOH (aqueous solution). The solution was given for 48 h into a closed

vessel which was tempered at 120°C hours. After that, the solution was washed with distilled water to achieve pH ~12. Then, the dispersion was neutralized by concentrated HCl to obtain pH 6–6.5. Finally, the samples were filtered and dried under the vacuum for 24 h. The dried nanotubes were studied via TEM. In Fig. 1 are shown the resulting nanotubes. The pictures demonstrate the formation of long, closed, and almost aggregation-free nanotubes.

2.2. Preparation of MMMs

PPO and PBI were used to prepare MMMs by solvent evaporation method. A pre-weighted amount of filler was then added to the polymer solution. The PPO–TiNT membranes were prepared by dissolving PPO in chloroform to obtain a 5% (w/w) casting solution. The solution was stirred with a magnetic stirrer till the polymer was dissolved. In the next step, the nanotubes were added and the solution was shaken till the nanotubes were well distributed. The content of TiNT in the membranes was 3, 6, and 9 wt.%, respectively. The casting solution was poured onto a clean glass surface, and the solvent was evaporated under air.

PBI–TiNT membranes were prepared using the commercial available PBI solution (dissolved in DMAc, 10% w/w) which was diluted with DMAc to obtain a 5% (w/w) casting solution. PBI solution was mixed with TiNT using a magnetic stirrer for 24 h. The TiNT content in the membranes was 1.5, 3, and 6 wt.%.

The casting solution was poured onto a clean glass surface, and the solvent was evaporated an oven (24 h, 65°C).

The dried films were stripped of in a tray of water and stored on a dry place prior to use. Residual solvent was removed in a vacuum oven at 60°C for 24 h.

2.3. Characterization and measurements

The size and morphology of TiNTs were analyzed using a TEM microscope Tecnai G Spirit (FEI, 120 kV).

For investigating the membrane cross-sectional morphology, the membranes were cracked in liquid nitrogen, coated with platinum, and observed using a Vega Plus TS 5135 (Tescan) scanning electron microscope.

Thermal stabilities of the MMMs were studied on Pyris 1 from PerkinElmer. The heating was performed in two steps. First step was at 110°C for 1 h to remove the vapor inside the matrix. Second step was the heating in the temperature range 50–900°C, at a heating rate of 20°C/min in a nitrogen purge (30 cm³/min).

ATR FTIR spectra were measured using a Thermo Nicolet NEXUS 870 FTIR spectrometer (Madison, WI, USA) in an H₂O-purged environment with MCT (mercury cadmium telluride) detector in the wavelength range from 400 to 4,000 cm⁻¹ to investigate the interaction between TiNTs with PBI and PPO, respectively. MKII Golden Gate™ Heated Diamond ATR Top-Plate single reflection system (Specac Ltd., Orprington, Great Britain) was applied for the measurements of

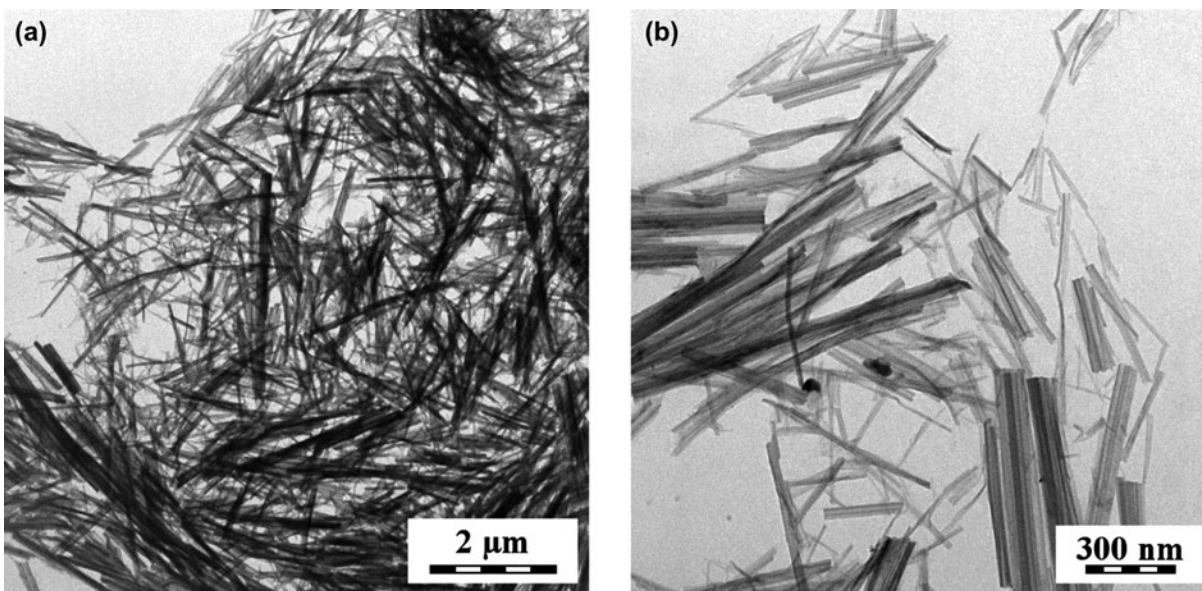


Fig. 1. TEM images of the TiNT with the scale (a) 2 μm and (b) 300 nm.

spectra of the samples. Typical parameters used are as follows: 256 of sample scans, resolution 4 cm^{-1} , Happ–Genzel apodization, KBr beamsplitter.

Gas permeability through membranes was determined using a laboratory time lag method high vacuum apparatus with a static permeation cell, which possess an effective membrane area of 1.24 cm^2 , at 30°C . The studied membrane was placed and sealed in a module which was over night at 30°C in the apparatus to degas the sample. Feed pressure p_i was 1.5 bar. The permeability P was determined from the increase of pressure Δp_p per time Δt in a calibrated volume V_p of the product part of the cell during steady state permeation. For calculation of permeability, the following formula was used (Eq. (1)) [17]:

$$P = \frac{\Delta p_p}{\Delta t} \cdot \frac{V_p \cdot l}{A \cdot p_i} \cdot \frac{1}{RT} \quad (1)$$

where l is the membrane thickness, S the area, T the temperature, and R the gas constant. Permeabilities are reported in units of Barrer ($1 \text{ Barrer} = 1 \times 10^{-10} \text{ cm}^3(\text{STP}) \text{ cm}/(\text{cm}^2 \text{ s cm Hg})$). All measurements were carried out at 30°C . In our experiments, gasses such as H_2 , O_2 , N_2 , CH_4 , and CO_2 were studied. Each gas possessed a purity of 99.99% and was used as received from Messer Technogas s.r.o. (Czech Republic). The selectivity α_{ij} of two gasses i and j was determined by the ratio (Eq. (2)) [17]:

$$\alpha_{i/j} = P_i/P_j \quad (2)$$

Sorption studies were conducted with the gravimetric system, IGA-002, Hiden Isochema, UK. Each sample was degassed at 50°C for 48 h at pressures below 10^{-6} mbar . All tubings and chambers were also degassed by applying a vacuum ($P \leq 10^{-6} \text{ mbar}$). The degassed samples were then cooled down to 30°C . The gasses used in this research were the same as for permeability measurements including water vapor. The adsorption isotherms were measured by stepwise pressure changes (pressure increase rate $100 \text{ mbar}/\text{min}$) within the pressure range of $0.01\text{--}6 \text{ bar}$.

3. Results and discussion

Investigation of TiNT distribution in the polymer matrix was examined by SEM. Cross sections of PBI membranes containing 0, 1.5, 3, and 6 wt.% of TiNT, respectively, and PPO samples with 0, 3, 6, and 9 wt.% of TiNT, respectively, were examined. It can be seen in both micrographs (Fig. 2(a) and (b)), the membranes are homogenous and the TiNT distribution in both materials is somewhat random and not aligned. Similar results were obtained for all other membranes and the neat polymer. Comparing the cross sections and the partially exhibited surfaces of the composite membranes, we observed that the nanotubes have a good adhesion to the polymer matrix.

In the infrared spectra of PBI–TiNT composites, some changes were observed with the increase of TiNT content (Fig. 3). It is concluded that TiNT interacts with PBI in the composite via N–H bonds present in the structure of PBI and the Ti–O groups present in TiNT. In case of PPO, there are no bonds in the

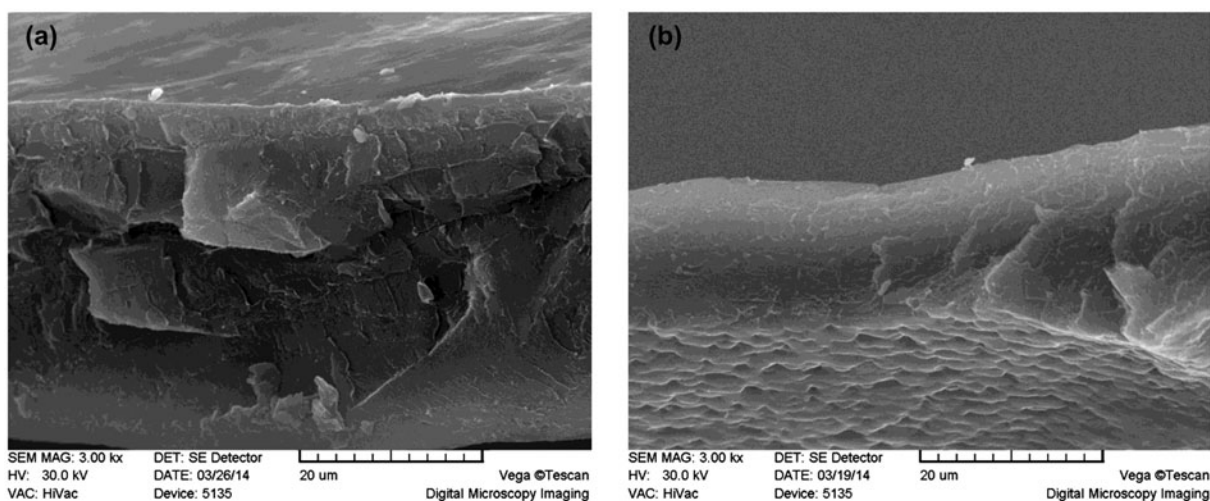


Fig. 2. Cross sections of the composite membranes (a) PBI–TiNT 6 wt.% and (b) PPO–TiNT 9 wt.%.

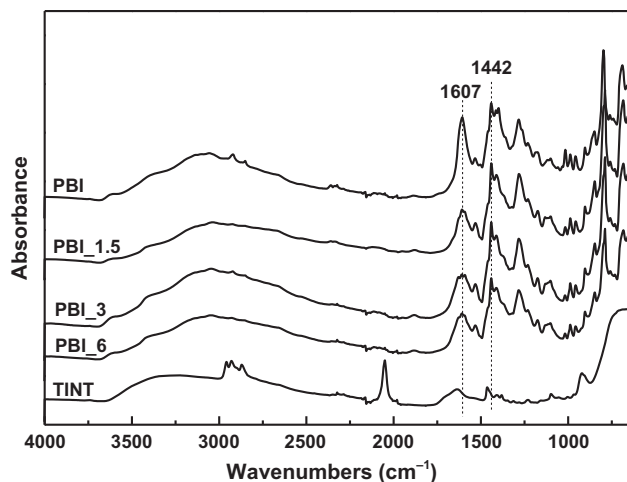


Fig. 3. Infrared spectra of PBI membrane and of the composites of PBI membrane with various amount of TiNT. Spectrum of pure TiNT is shown for comparison.

structure which are suitable for building hydrogen bonds with the groups present in TiNT.

Figs. 4 and 5 show the TGA plots of the prepared PPO and PBI MMMs. The TGA plot of PPO membranes revealed that TiNTs have no effect on the thermal stability of PPO composites due to the high stability of the neat PPO membrane. However, it increases the degradation temperatures and the onset of accelerated weight loss of the PBI composites compared to the pure PBI membrane; thus, implying that the thermal stability of the PBI–TiNT membranes was improved with the addition of the fillers, which is in accordance with other researches [18–21]. The onset temperatures, derivative peak maxima temperatures

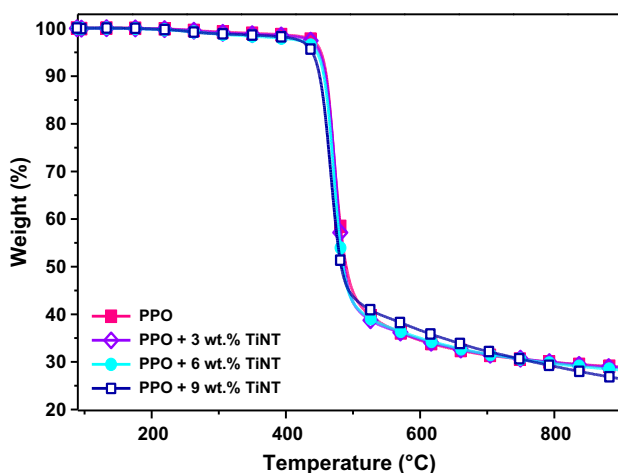


Fig. 4. TGA plot of PPO and PPO–TiNT membranes.

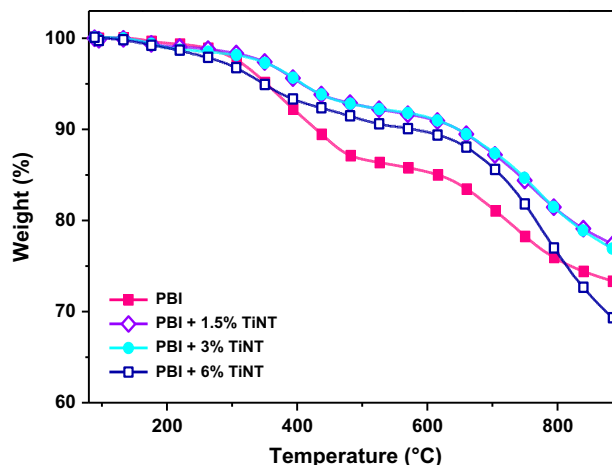


Fig. 5. TGA plot of PBI and PBI–TiNT membranes.

T_{max} , weight loss Δm , residue at 900°C $w_{R900^\circ C}$, temperature at which the weight loss is 5 or 10 wt. $T_{5\%}$ and $T_{10\%}$ are summarized in Table 1.

Dependence of permeability coefficients on the content of TiNT in PPO matrix is presented in Fig. 6(a). For all samples permeability coefficients decreased in the order: $H_2 > CO_2 > O_2 > CH_4 > N_2$ which indicates that the separation mechanism is based on sorption–diffusion mechanism. The permeability of all studied gases increases with the increase of TiNT concentration in the PPO matrix. This is probably due to lower adhesion between the TiNT and the PPO matrix, as FTIR results indicate (gas molecules can easily diffuse along the interfaces of both materials). Other explanation of increased permeabilities of TiNT/PPO membranes consists in the transport of gases through the free inner space of TiNT.

Fig. 6(b) shows ideal selectivities of selected gas pairs. A linear trend line, calculated via least square method, was added for each gas pair. Selectivity values for H_2/N_2 were somewhat scattered along the slightly rising linear trend line. Similarly, O_2/N_2 trend line was almost constant, that is, there is a negligible influence of TiNT addition on ideal selectivities. On the other hand, ideal selectivities for CO_2/CH_4 and CO_2/N_2 have decreasing tendency with higher content of TiNT in PPO matrix. Strongest decrease was observed for CO_2/CH_4 .

Based on a significant permeability increase at a relatively low change in selectivities, we can conclude that the presence of TiNT in PPO matrix has a positive effect on gas separation.

The dependence of permeability coefficients on the concentration of TiNT in PBI is presented in Fig. 7(a). The permeability coefficients for different

Table 1
TGA measurement results

	Onset temp. (°C)	$T_{\max 1}$ (°C)	Δm_1 (wt.%)	$T_{\max 2}$ (°C)	Δm_2 (wt.%)	$T_{\max 3}$ (°C)	Δm_3 (wt.%)	$W_{R900^\circ\text{C}}$ (wt.%)	$T_{5\%}$ (°C)	$T_{10\%}$ (°C)
PBI	246	169	0.6	343	13.2	714	13.2	73	353	430
PBI + 1.5% TiNT	234/320	166	0.9	399	7.1	735	14.8	77	409	652
PBI + 3% TiNT	273	–	–	339	8.8	782	22.4	68	351	587
PBI + 6% TiNT	306	172	1.3	399	6.4	767	15.5	77	411	650
PPO 104	449	471	64	–	–	–	–	29	452	–
PPO + 3% TiNT	448	474	64	–	–	–	–	29	450	–
PPO + 6% TiNT	447	471	62	–	–	–	–	28	445	–
PPO + 9% TiNT	437	468	60	–	–	–	–	27	439	–

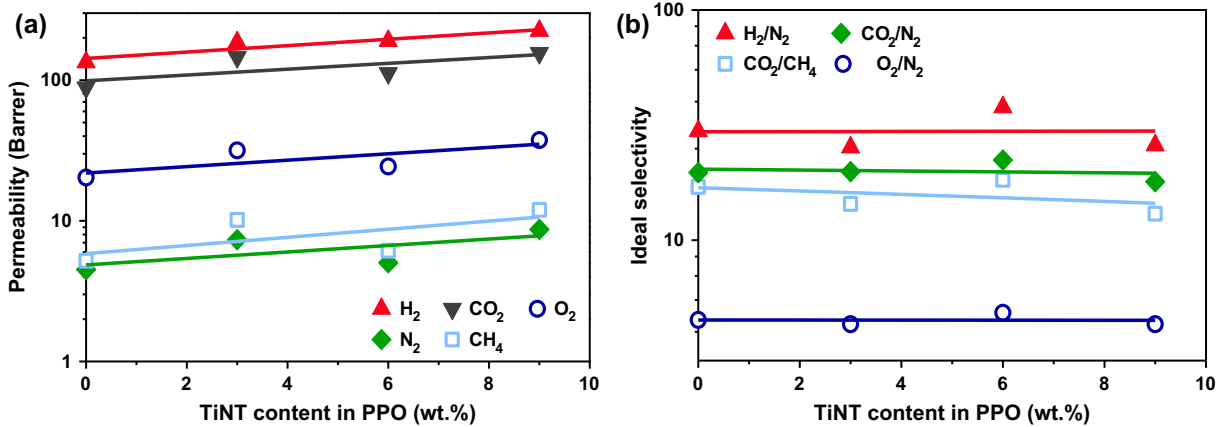


Fig. 6. Permeability coefficients (a) and ideal selectivities (b) of PPO and PPO-TiNT membranes for the gasses H₂, O₂, N₂, CO₂, and CH₄.

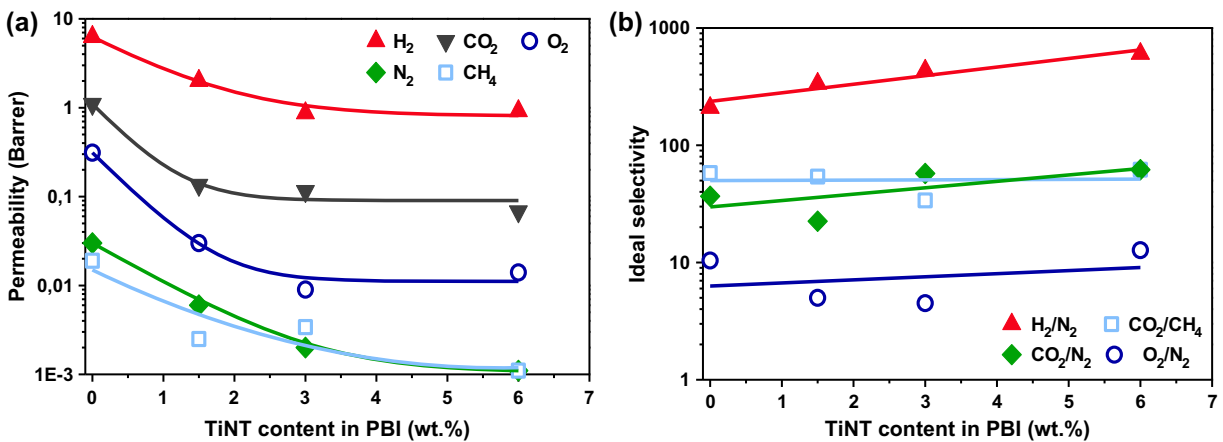


Fig. 7. Permeability coefficients (a) and ideal selectivities (b) of PBI and PBI-TiNT membranes for the gasses H₂, O₂, N₂, CO₂, and CH₄.

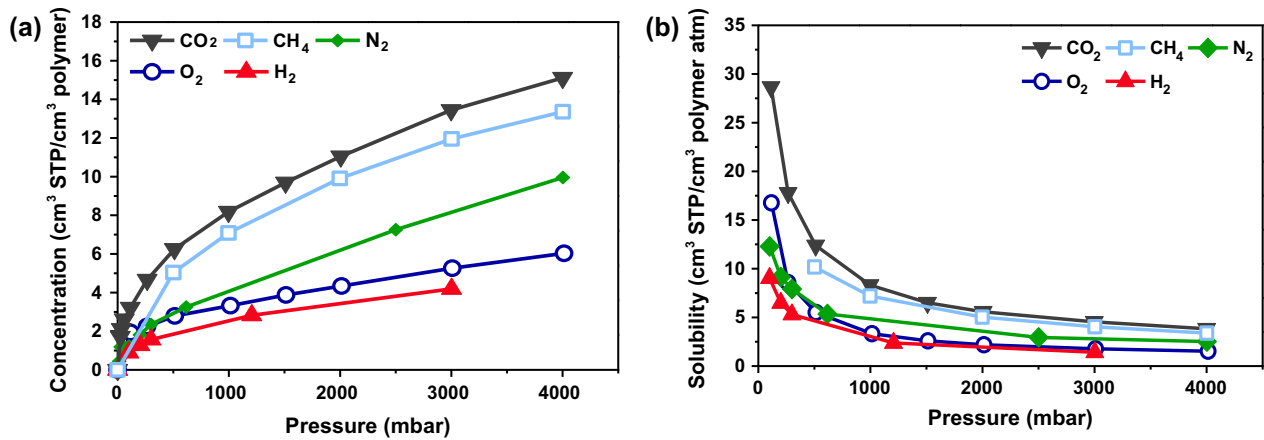


Fig. 8. Sorption isotherms (a) and solubility coefficients (b) of PBI measured at 30°C.

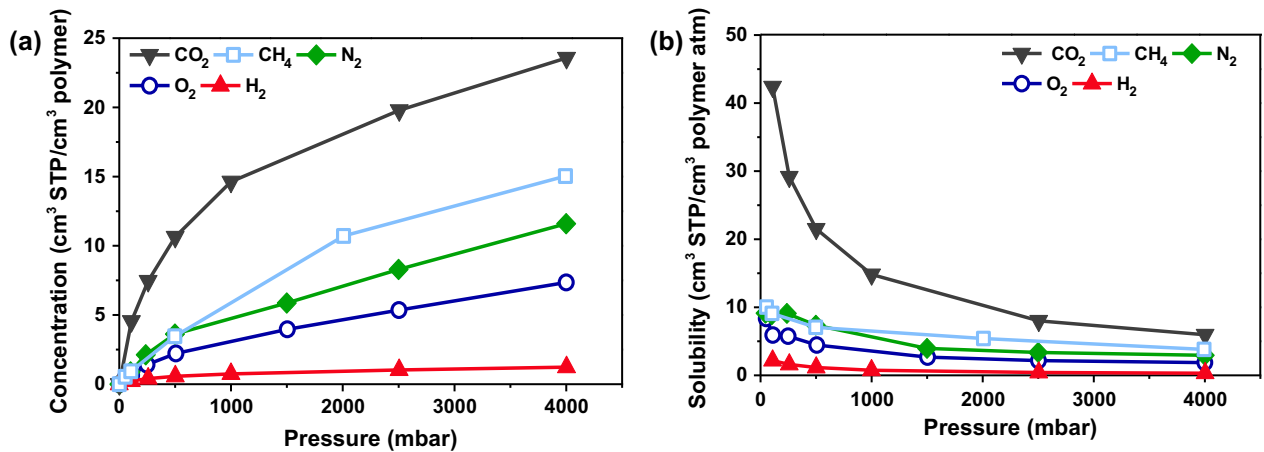


Fig. 9. Sorption isotherms (a) and solubility coefficients (b) of PBI-TiNT (6 wt.%) measured at 30°C.

gasses decreased in the same order as it was the case with the TiNT/PPO membranes, except for the pair CH₄/N₂. However, in this case, the values are so small that an experimental error cannot be ruled out. The permeability coefficients are here considerably lower than those of PPO membranes, and in addition to this, an addition of TiNT brought about a strong decrease in permeabilities.

Fig. 7(b) shows the dependence of ideal selectivities on TiNT content in PBI membranes. Plots were fitted with linear trend lines. The ideal selectivities are increasing with increasing TiNT content in PBI matrix. Significant increases were observed for a H₂/N₂ and CO₂/N₂ pairs.

Sorption isotherms and corresponding solubility coefficients of PBI are presented in Fig. 8(a) and (b). Sorption isotherms show concave shapes of curves suggesting dual-sorption behavior (Eq. (3)) which is typical for most glassy polymers [22].

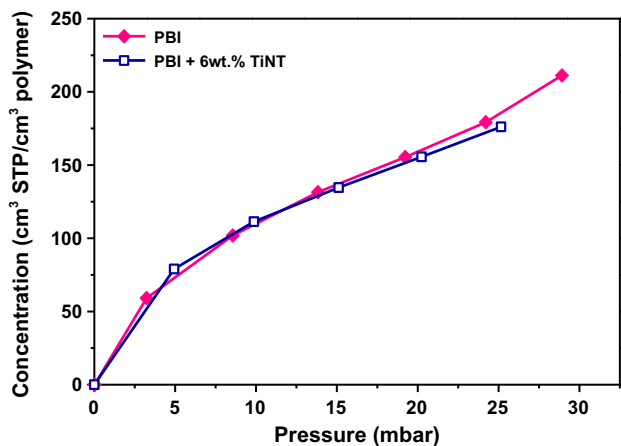


Fig. 10. Comparison of water vapor sorption isotherms of neat PBI and PBI with 6 wt.% measured at 30°C.

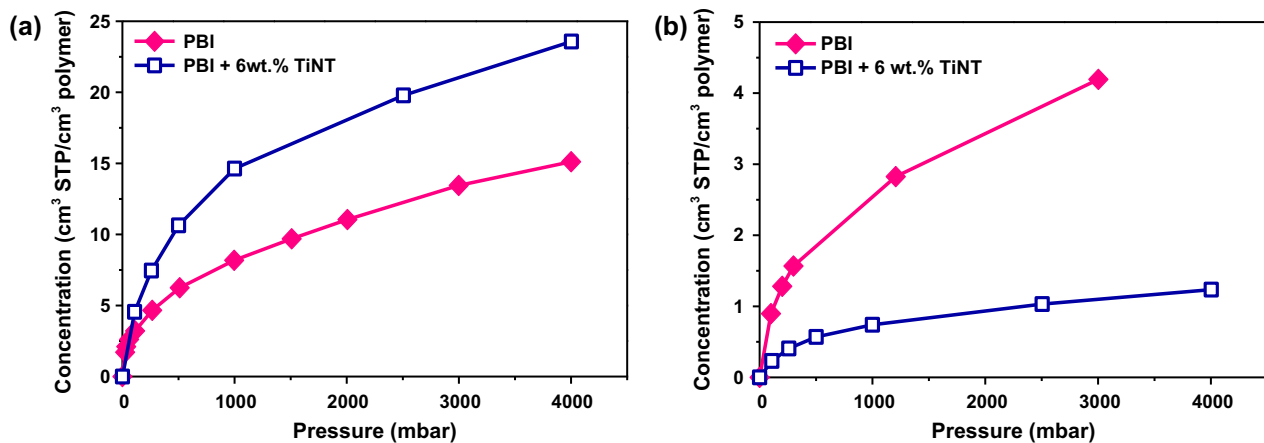


Fig. 11. Comparison of sorption isotherms of neat PBI and PBI with 6 wt.%: (a) for CO₂ and (b) for H₂, measured at 30°C.

$$C = k_D p + \frac{c_H b p}{1 + b p} \quad (3)$$

where k_D , c_H , and b are the Henry law, Langmuir capacity, and Langmuir affinity parameters, respectively. Gas sorbed according to Henry's law increases linearly with the pressure, while gas sorbed in the Langmuir mode has a capacity limit because it behaves like a hole-filling process. The lowest sorptions exhibit gasses with low condensability, such as H₂, O₂, and N₂. These gasses also show weak interactions with polymer materials. On the other hand, easily condensable gasses such as CO₂ and CH₄ exhibit significantly higher sorptions than the gasses with low condensability. It can be seen in PBI sorption isotherms that at pressures above 1.5 bar, all curves become linear with increasing pressure. This suggests Henry law sorption solubility coefficients, defined as $S = C/p$ tends to decrease with increasing pressure.

Similar behavior was observed also for sorption isotherms and corresponding solubility coefficients of PBI/6 wt.% TiNT which are presented in Fig. 9.

Comparison of water vapor sorption isotherms of neat PBI and PBI with 6 wt.% showed very high sorptions about 200 (cm³ STP/cm³ polymer) but negligible influence of TiNT on sorption (Fig. 10). No influence on sorptions was also observed on CH₄.

In Fig. 11 is presented comparison of sorption isotherms of neat PBI and PBI with 6 wt.% TiNT for CO₂ and H₂. It can be clearly seen that presence of TiNT nanotubes considerably increases the sorption of CO₂ (Fig. 11(a)). Similar increase was observed also for N₂

and O₂. This could be attributed to a high polarity of TiNT but also probably to an accessibility of inner nanotube surface where sorption can take place. On the other hand, the presence of TiNT in PBI has negative effect on H₂ sorptions as can be seen in Fig. 11(b).

The comparison of permeability and sorption data of CO₂ proposes that the CO₂ molecules preferably adsorb on TiNT surface due to the simultaneous decrease of CO₂ permeation and increase of CO₂ sorption with the increase of TiNT content (Figs. 7(a) and 11(a)).

4. Conclusions

- (1) TiNT can be incorporated in PBI and in PPO. The obtained blends can be used for the preparation of MMMs with a homogeneous structure.
- (2) While PBI and TiNT interact possibly via hydrogen bonds, no interactions between PPO and TiNT were observed.
- (3) An increase in TiNT concentration in PBI/TiNT membrane leads to a decrease in gas permeabilities and an increase in gas selectivities.
- (4) An increase in TiNT concentration in PBI/PPO membrane leads to an increase in gas permeabilities and a decrease in gas selectivities.
- (5) Sorption isotherms of PBI in PBI/TiNT showed dual-sorption mechanism for most of the studied gasses.

Acknowledgments

This work was supported by the Grant Agency of the Czech Republic for financial support of the study (grant P106/12/P643). Infrastructure of Membrane Innovation Centre (No. CZ 1.05/2.1.00/03.0084) was utilized for membrane casting. We would like to thank our colleagues of the other departments for providing the nanotubes and for the help with TEM images.

List of symbols

A	—	membrane area
b	—	Langmuir affinity constant
C	—	total gas concentration
c_H	—	Langmuir capacity constant
k_D	—	Henry's constant
l	—	membrane thickness
P	—	permeability
p	—	penetrant partial pressure
p_i	—	feed pressure
p_p	—	pressure increase, mbar
R	—	ideal gas constant
S	—	solubility coefficient
T	—	temperature
t	—	time
V_p	—	volume of the product part

Greek symbol

α	—	selectivity
----------	---	-------------

References

- [1] P. Bernardo, E. Drioli, G. Golemme, Membrane gas separation: A review/state of the art, *Ind. Eng. Chem. Res.* 48 (2009) 4638–4663.
- [2] L.M. Robeson, Correlation of separation factor versus permeability for polymeric membranes, *J. Membr. Sci.* 62 (1991) 165–185.
- [3] S. Kim, High Permeability/High Diffusivity Mixed Matrix Membranes for Gas Separations, Dissertation, Virginia Polytechnic Institute, 2007.
- [4] D. Bastani, N. Esmaili, M. Asadollahi, Polymeric mixed matrix membranes containing zeolites as a filler for gas separation applications: A review, *J. Ind. Eng. Chem.* 19 (2013) 375–393.
- [5] S. Kim, T.W. Pechar, E. Marand, Poly(imide siloxane) and carbon nanotube mixed matrix membranes for gas separation, *Desalination* 192 (2006) 330–339.
- [6] G. Clarizia, C. Algieri, E. Drioli, Filler-polymer combination: A route to modify gas transport properties of a polymeric membrane, *Polymer* 45 (2004) 5671–5681.
- [7] A.E. Rogacheva, A.P. Kharitonov, A.S. Vinogradov, V.V. Teplyakov, Gas permeability properties of modified membranes based on exfoliated graphite, *Desalin. Water Treat.* 14 (2010) 192–195.
- [8] B. Zornoza, P. Gorgojo, C. Casado, C. Téllez, J. Coronas, Mixed matrix membranes for gas separation with special nanoporous fillers, *Desalin. Water Treat.* 27 (2011) 42–47.
- [9] P. Sysel, E. Minko, M. Hauf, K. Friess, V. Hynek, O. Vopicka, K. Pilnacek, M. Sipek, Mixed matrix membranes based on hyperbranched polyimide and mesoporous silica for gas separation, *Desalin. Water Treat.* 34 (2011) 211–215.
- [10] V.N. Popov, Carbon nanotubes: Properties and application, *Mater. Sci. Eng., R* 43 (2004) 61–102.
- [11] K. Sears, L. Dumée, J. Schütz, M. She, C. Huynh, S. Hawkins, M. Duke, S. Gray, Recent developments in carbon nanotube membranes for water purification and gas separation, *Materials* 3 (2010) 127–149.
- [12] A. Sharma, B. Tripathi, Y.K. Vijay, Dramatic improvement in properties of magnetically aligned CNT/polymer nanocomposites, *J. Membr. Sci.* 361 (2010) 89–95.
- [13] H. Cong, J. Zhang, M. Radosz, Y. Shen, Carbon nanotube composite membranes of brominated poly(2,6-diphenyl-1,4-phenylene oxide) for gas separation, *J. Membr. Sci.* 294 (2007) 178–185.
- [14] T. Sekino, *Inorganic and Metallic Nanotubular Materials*, Springer-Verlag, Berlin Heidelberg, 2010, pp. 17–32.
- [15] B.V. d. Bruggen, The separation power of nanotubes in membranes: A review, *Int. Scholarly Res. Network ISRN Nanotechnol.* 2012 (2012) 1–17.
- [16] D. Kralova, M. Slouf, M. Klementova, R. Kuzel, I. Kelnar, Preparation of gram quantities of high-quality titanate nanotubes and their composites with polyamide 6, *Mater. Chem. Phys.* 124 (2010) 652–657.
- [17] J. Crank, *The Mathematics of Diffusion*, Oxford Press, London, 1990.
- [18] E.L. Vivas, A.B. Beltran, H.R. Cascon, J. Ahn, E.S. Cho, W.J. Chung, Inorganic filler selection in PDMS membrane for acetone recovery and its application in a condenser-gas membrane system, *Desalin. Water Treat.* 17 (2010) 160–167.
- [19] F.M. Nor, I. Abdullah, R. Othaman, Gas permeability of ENR/PVC membrane with the addition of inorganic fillers, *AIP Conf. Proc.* 1571 (2013) 911–917.
- [20] E. Quartarone, P. Mustarelli, A. Carollo, S. Grandi, A. Magistris, C. Gerbaldi, PBI composite and nanocomposite membranes for PEMFCs: The role of the filler, *Fuel Cells* 9 (2009) 231–236.
- [21] Surzani, C.-M. Chang, Y.-L. Liu Y.M. Lee, Polybenzimidazole membranes modified with polyelectrolyte-functionalized multiwalled carbon nanotubes for proton exchange membrane fuel cells, *J. Mater. Chem.* 21 (2011) 7480–7486.
- [22] D.R. Paul, Gas sorption and transport in glassy polymers, *Chem. Phys.* 83 (1979) 294–302.